Journal of the Serbian Chemical Society
JSCS-info@shd.org.rs • www.shd.org.rs/JSCS
J. Serb. Chem. Soc. *84* (3) 277–291 (2019)
JSCS–5183
UDC 546.562'472+519.677:547.963.32+547.853:615.277
Original scientific paper

Computational, antimicrobial, DNA binding and anticancer activities of pyrimidine incorporated ligand and its copper(II) and zinc(II) complexes

MURUGESAN SANKARGANESH[1], NAGARAJ REVATHI[2,3], JEYARAJ DHAVEETHU RAJA[1]*, KARUNGANATHAN SAKTHIKUMAR[1], GUJULUVA GANGATHARAN VINOTH KUMAR[1], JEGATHALAPRATHABAN RAJESH[1], MANIKKAM RAJALAKSHMI[4] and LIVIU MITU[5]**

[1]*Chemistry Research Centre, Mohamed Sathak Engineering College, Kilakarai, Ramanathapuram, Tamil Nadu 623 806 India,* [2]*Department of Chemistry, Ramco Institute of Technology, Rajapalayam, Virudhunagar, Tamil Nadu 626 117, India,* [3]*Department of Chemistry, Manonmanium Sundaranar University, Tirunelvi, Tamil Nadu 627 012, India,* [4]*Bioinformatics Centre, PG & Research Centre Department of Biotechnology and Bioinformatics, Holy Cross College (Autonomous), Tiruchirapalli, Tamil Nadu 620 002, India and* [5]*Department of Nature Sciences, University of Pitesti, Pitesti 110 040, Romania*

(Received 6 June, revised 7 August, accepted 5 September 2018)

Abstract: In this research article, the synthesis, structural characterization, and biological, DNA binding and anticancer properties of pyrimidine incorporated Schiff base ligand **L** and its $[CuL_2](ClO_4)_2$ (**1**) and $[ZnL_2](ClO_4)_2$ (**2**) complexes are reported. The isolated complexes **1** and **2** have significant antibacterial and antifungal properties, greater than those of ligand **L**. The interaction between protein and **L** were analyzed by an *in silico* method. The intercalative binding of the prepared compounds was proved from electronic absorption, fluorometric, cyclic voltammetric and viscometric methods. The calculated binding parameters such as, K_b (2.65×10^3, **L**; 7.74×10^3, **1** and 2.99×10^3, **2**); K_{sv} (3.30×10^3, **L**; 4.31×10^3, **1** and 3.89×10^3, **2**), and K_{app} (2.15×10^5, **L**; 3.30×10^5, **1** and 2.82×10^5, **2**) indicted that complex **1** has better interaction ability than **L** and complex **2**. The *in vitro* anticancer properties of **L**, and complexes **1** and **2** against human cancer (MCF-7, HeLa and HEp-2) and normal (NHDF) cell lines were determined by the MTT assay method. The obtained results designated that complexes **1** and **2** exhibited substantial anticancer activity against the cancer cell lines, better than that of **L**.

Keywords: metal complexes; DFT; antimicrobial; DNA interaction; anticancer studies.

*,** Corresponding authors. E-mail: (*)jdrajapriya@gmail.com; (**)ktm7ro@yahoo.com
https://doi.org/10.2298/JSC180609080S

INTRODUCTION

Pyrimidine is a heterocyclic compound and it forms the backbone of deoxyribonucleic acid (DNA) and ribonucleic acid (RNA). Pyrimidine derivative drugs reveal various pharmacological and biological activities, such as, antitumor,[1,2] antiamoebic,[3] antimalarial,[4,5] antipneumocystis carinii pneumonia[6] and antimicrobial.[2,7,8] Moreover, the attachment of CF_3 groups results in compounds that are lipophilically and pharmacologically more active than the corresponding non-fluorinated compounds. These $–CF_3$-substituted organic compounds have various biological competences, such as, herbicidal, fungicidal, analgesic, antihyperglycemic and antipyretic, *etc.*[9–13] Pyrimidine-containing drugs, such as gefitinib, erlotinib and afatinib were used in cancer-related treatments.[14] Therefore, Schiff base ligands were prepared from biologically and pharmacologically active pyrimidine derivative compounds. These Schiff base ligands possess analytical, biological and pharmacological applications.[15] In earlier days, Schiff bases were employed to develop metal-based complexes[16,17] because metal complexes acquire diverse biological abilities, such as antidiabetic, antimicrobial, antioxidant, DNA cleavage or binding and anticancer activities.[18–20] Especially, copper(II) and zinc(II) complexes were synthesized with much more interest due to their enhanced biological applications.[21–23]

The interest in the biological properties of copper(II) and zinc(II) complexes has been continued in the present study through incorporation of a bio-active pyrimidine ligand. The formations of **L**, and complexes **1** and **2** were confirmed from analytical, spectroscopic and theoretical techniques. Moreover, their biological properties, such as antimicrobial, DNA binding and *in vitro* anticancer activities were studied.

EXPERIMENTAL

Materials and methods

4-(4-Morpholinyl)benzaldehyde, 2-hydrazino-4-(trifluoromethyl)pyrimidine, Tris-HCl, sodium chloride and ethidium bromide were procured from Sigma Aldrich. $Cu(ClO_4)_2·6H_2O$ and $Zn(ClO_4)_2·6H_2O$ were received from Alfa Aesar company. Calf thymus (CT) DNA was purchased from GeNei Bangalore, India. Elemental analyses were realized on an Elementar Vario EL III analyzer. FTIR and NMR spectra were recorded using an FTIR Affinity-1 Shimadzu instrument and Bruker (400 and 125 MHz) spectrometers. The mass spectra were obtained on an ESI-MS spectrometer. The ESR spectra were recorded at 300 and 77 K in an IIT, Mumbai. Cyclic voltammetric studies were recorded on a CHI650C instrument. The absorption and fluorescence spectra were recorded on a UV-1800 Shimadzu spectrophotometer and FluoroMax-4 spectrometer, HORIBA, respectively.

Analytical and spectral data are given in Supplementary material to this paper.

*Synthesis of ligand **L***

Ligand **L** was synthesized by refluxing 4-(4-morpholinyl)benzaldehyde (0.1912 g, 1 mmol) with 2-hydrazino-4-(trifluoromethyl)pyrimidine (0.1781 g, 1 mmol) in 25 mL of ethanol for 6 h. The resulting solution was slowly evaporated on a water bath. The yellow col-

oured product was collected by filtration and washed with 10 mL of cold methanol and recrystallized from hot chloroform.

*Synthesis of complexes **1** and **2***

An ethanolic solution of ligand **L** (2 mmol) was mixed with metal perchlorates (1 mmol) in 10 mL of ethanol maintaining a metal : ligand ratio of 1 : 2. The resulting solution was refluxed under stirring for 5 h. Then the solution was evaporated on a water bath, the precipitated solid filtered and washed thoroughly with 10 mL of petroleum ether and dried in *vacuo* over $CaCl_2$.

Computational studies

Density functional theory (DFT) calculations were performed with the hybrid exchange--correlation function using the 6-311G(d,p) and LANL2DZ basis set by the Gaussian 09 program to understand the mode of complexation between the ligand and its complexes.[24] Initially, the optimized geometries of both the ligand and its complexes were determined by the B3LYP functional but using 6-311G(d,p) and LANL2DZ basis set, respectively.

Antimicrobial studies

The antimicrobial activity of the prepared compounds were screened against the bacterial species, *Escherichia coli*, *Klebsiella pneumoniae*, *Pseudomonas fluorescens*, *Shigella sonnei* and *Staphylococcus aureus*, and the fungal species, *Aspergillus niger*, *Candida albicans*, *C. tropicalis, Mucor indicus* and *Rhizopus* by the well diffusion method.[21] The reference drugs streptomycin and amphotericin were used for the antibacterial and antifungal studies, respectively.

Anticancer studies

The anticancer capabilities of ligand **L**, complexes **1** and **2** against various cancer cell lines (MCF-7, breast adenocarcinoma; HeLa, cervical, HEp-2, laryngeal) and a single normal cell line (NHDF, normal human dermal fibroblasts) were performed by the MTT assay[25]:

$$\text{Inhibition, \%} = 100 - 100\frac{\text{Absorbance of sample}}{\text{Absorbamce of control}} \quad (1)$$

Protein–ligand docking

The docking of ligand **L** with protein was studied by a previously reported method.[26] The prepared proteins and ligand **L** were docked using the LibDock module of Accelrys Discovery Studio software, version 2.1, to acquire the drug with protein interaction.

DNA interaction

The CT-DNA interaction of ligand **L** and complexes **1** and **2** in 5 mM and 50 mM Tris-HCl buffer solution, respectively, under physiological conditions were appraised using absorption spectroscopy and fluorescence, cyclic voltammetric and viscometric measurements.[27-29]

RESULTS AND DISCUSSION

The synthetic route to ligand **L**, and complexes **1** and **2** are depicted in Schemes 1 and 2, respectively. The ligand **L** (4-(4-morpholinyl)benzaldehyde, 2--[4-(trifluoromethyl)-2-pyrimidinyl]hydrazone) is lemon yellow in colour and well soluble in acetone, acetonitrile, DMSO and DMF solvents. The complexes **1** and **2** are brown and dark brown colour and soluble in DMSO and DMF solvents. The molar conductance at infinite dilution (Λ_m) of complexes **1** and **2** in DMSO

was found at 104 Ω^{-1} cm^2 mol^{-1} for complex **1** and 109 Ω^{-1} cm^2 mol^{-1} for complex **2**, which signified them to be electrolytes. Moreover, the obtained conductance values confirmed that percholarate ions are present in the outside coordination sphere of complexes **1** and **2**.

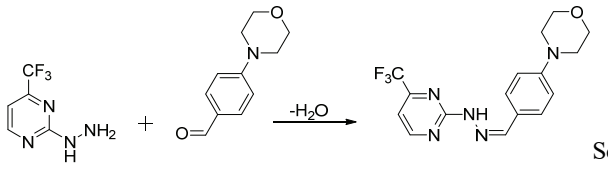

Scheme 1. Synthesis of ligand **L**.

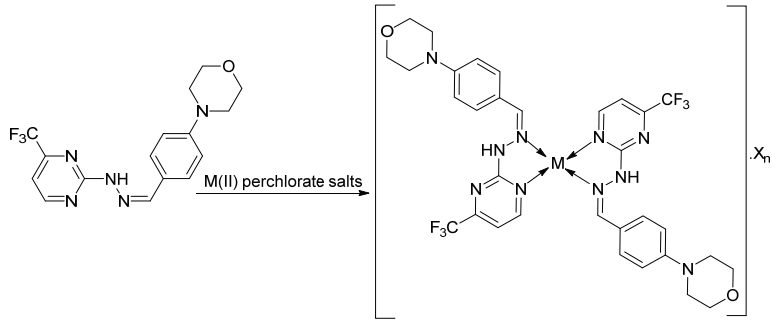

Scheme 2. Synthesis of complexes **1** and **2**.

NMR spectra

The ^{1}H-NMR spectra of ligand **L** and complex **2** were recorded in DMSO-d_6 solution (Supplementary material). In the ^{1}H-NMR spectrum of ligand **L**, the azomethine (–CH=N–) proton signal appeared at 8.10 (1H, *s*) and the NH proton signal at 9.90 (1H, *s*) ppm. The pyrimidine (–CH=C–CF_3 and =CH–N=) protons signals were observed at 7.19 (1H, *d*) and 8.77 (1H, *d*) ppm, respectively. The signals of the aromatic protons were found at 6.99 (2H, *d*) and 7.55 (2H, *d*) ppm. The morpholine moiety protons (mor-CH_2–N–CH_2– and mor-CH_2–O–CH_2–) signals appeared at 3.20 (4H, *t*) and 3.75 (4H, *t*) ppm, respectively.

In the ^{1}H-NMR spectra of complex **2**, the signals of the azomethine (–CH=N–) and pyrimidine moiety protons (=CH–N=) appeared at 8.64 (1H, *s*) and 8.83 (1H, *d*), respectively. These spectral results reveal that the azomethine and pyrimidine nitrogen atoms participate in the complexation. As per comparison with the free ligand **L**, the signals of the pyrimidine (–CH=C–CF_3 and –NH), aromatic and morpholine (mor-CH_2–N–CH_2– and mor-CH_2–O–CH_2–) protons remained more or less at the same positions in complex **2**.

The ^{13}C-NMR spectra of ligand **L** and complex **2** were taken in DMSO-d_6 solution and the obtained data are given in the Supplementary material. In the

spectra of ligand **L**, the azomethine (–CH=N), pyrimidine C_2 and C_6 appeared at 138.60, 160.61 and 153.60 ppm, respectively. In complex **2**, these peaks appeared at 139.45, 161.10 and 154.16 ppm, respectively. These results indicate that ligand **L** formed coordinate bonds with the central metal atom *via* azomethine and pyrimidine ring (C_2) nitrogen atoms.

FT-IR spectra

The FT-IR spectrum of ligand **L** showed a characteristic band at 1544 cm^{-1} due to ν(–CH=N) stretching vibrations.[30] The bands at 1591, 1465 and 1402 cm^{-1} are associated with ν(–NH) and ν(=CH–N=) aromatic ring nitrogen stretching vibrations, respectively. In the spectra of complexes **1** and **2**, characteristic bands appeared at 1522 (**1**) and 1535 cm^{-1} (**2**), and 1388 (**1**) and 1384 cm^{-1} (**2**), which are due to ν(CH=N) and ν(aromatic, =CH–N=) group vibrations. This result indicates that nitrogen atoms of azomethine ν(CH=N) and the pyrimidine ring ν(aromatic, =CH–N=) participated in the complexation. Bands are observed at 1087 and 1088 cm^{-1} in complexes **1** and **2**, respectively, due to the presence of perchlorates in the outer coordination spheres.

Mass spectra

In the ESI-MS spectrum of ligand **L**, the molecular ion peak was observed at *m*/*z* 350.9 and daughter peaks were observed for $C_{12}H_7N_4F_3^+$, $C_6H_5N_4F_3^+$ and $C_5H_4N_3F_3^+$. In complexes **1** and **2**, molecular ion peaks were obtained at *m*/*z*, 765 (**1**) and 767 (**2**). These values evidence that one mole of complex **1** or **2** contained with two moles of ligand **L**.

Electronic absorption spectra

In the UV–Vis spectra of ligand **L**, and complexes **1** and **2**, bands were observed at 266 and 336 nm owing to π→π* and n→n* transitions of ligand **L**.[31] The ligand to metal charge transfer (LMCT) spectra of complexes **1** and **2** showed bands at 272 and 329 nm for complex **1** and 270 and 338 nm for complex **2**. In the UV–Vis spectrum of complex **1**, a broad band was displayed at 777 nm and the band assignments are $^2B_{1g}\rightarrow{}^2A_{1g}$, $^2B_{1g}\rightarrow{}^2B_{2g}$ and $^2B_{1g}\rightarrow{}^2E_g$ transitions in a square planar arrangement.[32] Complex **2** possess d^{10} electronic configuration, which authenticates the absence of a d–d transition, and therefore complex **2** showed INCT bands at 270 and 338 nm, which confirms the complexation.

ESR spectra

ESR spectral data give knowledge of the environment of a metal ion. The ESR spectrum data of complex **1** recorded in DMSO at liquid nitrogen temperature gave g_{II} and g_I values of 2.35 and 2.07, respectively. The spectrum of complex **1** showed that *g*-tensor value are $g_{II} > g_I > 2.0027$, indicating the unpaired electrons lie predominantly in the d_{x^2}–d_{y^2} orbital, which suggests square

planar geometry around the central metal ion.[33–36] The g_{II}/A_{II} value is useful for predicting the structure of the complex **1** and the value of 154 suggests square planar arrangement of complex **1** around the central metal ion.[37] According to Hathaway and Billing,[38–40] the *G* value greater than 4 suggested that the local tetragonal axes are aligned parallel or only slightly misaligned.

Computational studies

The 3D structure of ligand **L**, and complexes **1** and **2** were optimized using Density functional theory (DFT) calculations accomplished through the (B3LYP/ /6-311G(d,p)/LANL2DZ) basis set using the Gaussian 09 program.[24] The basis set 6-311G(d,p) was used for the N, O, C and H atoms and LANL2DZ was exploited for complexes **1** and **2**. In ligand **L**, the HOMO is spread over the whole π-moiety, while the LUMO is spread over the pyrimidine and imine moieties. After the introduction of Cu(II), the HOMO is spread over the surrounding of the metal ion and its LUMO is spread on the pyrimidine moiety with little contribution of the metal ion. Similarly, in **2**, the HOMO and LUMO are more spread over the pyrimidine moiety and slightly in the morpholine moiety with a metal ion contribution (Fig. 1). In addition, the calculated HOMO–LUMO energy gap for complexes **1** and **2** was lower than that for the free ligand. The order of the energy band gap is **L** > **2** > **1**. The obtained results obviously indicate that the complexation of Cu(II) and Zn(II) to the ligand **L** result in a disruption of internal charge transfer, which may be responsible for the appearance of new absorption band in the visible region.

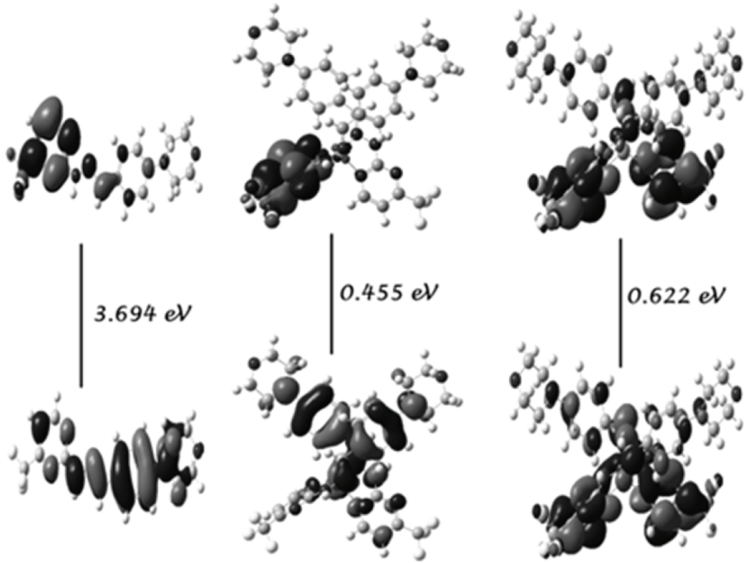

Fig. 1. Frontier molecular orbitals of Ligand **L**, complexes **1** and **2** (from left to right).

Biological studies

The pharmacological, DNA binding and *in vitro* anticancer activities of ligand **L**, complexes **1** and **2** were studied as follows.

Antimicrobial studies. The antimicrobial activity of ligand **L**, and complexes **1** and **2** were screened against the bacterial species *E. coli*, *K. pneumoniae*, *P. fluorescens*, *S. sonnei* and *S. aureus*, and the fungal species *A. niger*, *C. albicans*, *C. tropicalis, M. indicus* and *Rhizopus*. The reference drugs streptomycin and amphotericin were used for the antibacterial and antifungal studies, respectively. The zone of inhibition values of isolated compounds are presented in Table I. The obtained results established that the synthesized complexes **1** and **2** acted as better antibacterial and antifungal agents than ligand **L** due to their chelation ability.[41] Additionally, ligand **L**, and complexes **1** and **2** show superior activity against *E. coli* bacteria and *C. albicans* fungi than against the other pathogens.

TABLE I. Antimicrobial activities (zone of inhibition, mm) of ligand **L**, and complexes **1** and **2**

Compound	Bacterial strains				
	E. coli	*K. pneumoniae*	*P. fluorescens*	*S. sonnei*	*S. aureus*
1	9	8	8	8	8
2	8	6	6	7	6
L	6	5	4	5	4
Streptomycin	18	12	14	16	16
	Fungal strains				
	A. niger	*C. albicans*	*C. tropicalis*	*M. indicus*	*Rhizopus*
1	9	15	12	7	9
2	8	13	9	6	8
L	5	10	6	5	6
Amphotericin	18	17	31	9	24

Anticancer studies. The positive results received from the biological studies encouraged the investigation of the anticancer ability of the pyrimidine incorporated compounds. The *in vitro* anticancer activities of the ligand **L**, and complexes **1** and **2** against human cancer cell lines (MCF-7, breast adenocarcinoma; HeLa, cervical; HEp-2, laryngeal) and NHDF (normal human dermal fibroblasts) cell line were examined by using the MTT assay (Fig. S-1). The 50 % inhibitory concentration (IC_{50}, μg mL^{-1}) values of the prepared compounds against human normal and cancer cell lines are given in Table II. From the obtained data, cisplatin can affect the cancer as well as normal cell lines at lower concentration (6.93±0.35 μg mL^{-1} MCF-7; 7.46±0.37 μg mL^{-1} HeLa; 10.28±0.51 μg mL^{-1} HEp-2). When compared to the above results, **L** had no significant anticancer activity against the cancer cell lines or the normal cell lines (75.82±3.79 μg mL^{-1} MCF-7; 76.26±3.81 μg mL^{-1} HeLa; 81.03±4.05 μg mL^{-1} HEp-2). Moreover, the IC_{50} values of the complexes **1** and **2** against cancer cell lines revealed that

complex **1** has moderate anticancer ability on MCF-7 (54.51±2.73 μg mL^{-1}) and on HeLa (55.40±2.77 μg mL^{-1}) cell lines which was not so obvious on the HEp-2 cell line (77.57±3.88 μg mL^{-1}). However, complex **2** expressed modest anticancer activities on all three selected cancer cell lines (58.89±2.94 μg mL^{-1}, MCF-7; 59.98±2.99 μg mL^{-1}, HeLa; 60.79±3.04 μg mL^{-1}, HEp2). From these observations, the pyrimidine incorporated complexes **1** and **2** could control the growth of cancer cells.

TABLE II. Anticancer activities of ligand **L**, and complexes **1** and **2** on cancer and normal cell lines

Compound	IC_{50} / μg mL^{-1}			
	MCF-7	HeLa	HEp-2	NHDF
Cisplatin	6.93±0.35	7.26±0.36	7.46±0.373	10.28±0.51
L	75.82±3.79	76.26±3.81	81.03±4.05	100.48±5.02
1	54.51±2.73	55.40±2.77	77.57±3.88	105.67±5.28
2	58.89±2.94	59.98±2.99	60.79±3.04	107.04±5.35

Protein–ligand interaction

The mode of interaction of ligand **L** with antioxidant enzymes and the estrogen receptor alpha was analyzed using molecular docking studies. From the various obtained docked poses, the best pose was chosen based on the higher absolute energy and the LibDock score. The protein–ligand interaction was found to be stronger in the presence of hydrogen bond interactions, especially with bond length less than 0.3 nm (Table III).[42,43] The present study also revealed the presence of H-bond interaction between ligand **L** and the proteins indicating a better protein–ligand interaction. Binding of ligand **L** with the antioxidant enzymes and the estrogen receptor alpha predicts the mode of action through which the compound acts as an anticancer agent by regulating their involvement in cancer progression.

TABLE III. *In silico* results for protein–ligand interactions

Interaction of ligand L with	No. of poses	Absolute energy, kcal[a] mol^{-1}	Libdock score, kcal mol^{-1}	No. of H-bonds	Bond length, nm	Interacting residues
1SPD_A	12	74.225	60.174	1	0.24	VAL 81
1QQW_A	25	74.426	112.491	1	0.23	TYR 358
2HE3_A	19	74.426	101.122	1	0.25	SER 132
1A52_A	67	74.669	97.379	4	0.240	ARG 394

[a]1 kcal = 4184 J

DNA binding

Absorption titration. The interaction between the compounds and CT-DNA was ascertained by electronic absorption spectroscopy. The absorption spectra of complexes **1** and **2** (50 μM) in the presence and absence of CT-DNA (0–50 μM)

were assessed by typical absorption spectral titrations (Fig. 2a and b). As shown in Fig. 2a and 2b, the incremental addition of CT-DNA to solutions of complex **1** and **2** led to hypochromism (6.27, **L**; 15.60, **1** and 13.57, **2**) with bathochromic shifts of 3–6 nm. These observed spectral titration results clearly indicate that complexes **1** and **2** can bind with CT-DNA through intercalative interaction due to the presence of the pyrimidine substituent. In order to determine the intrinsic binding constants (K_b) of the prepared compounds, the following equation[25] was used:

$$\frac{c_{DNA}}{\varepsilon_a - \varepsilon_f} = \frac{c_{DNA}}{\varepsilon_b - \varepsilon_f} + \left[K_b\left(\varepsilon_b - \varepsilon_f\right)\right]^{-1} \quad (2)$$

where c_{DNA} is the concentration of CT–DNA.

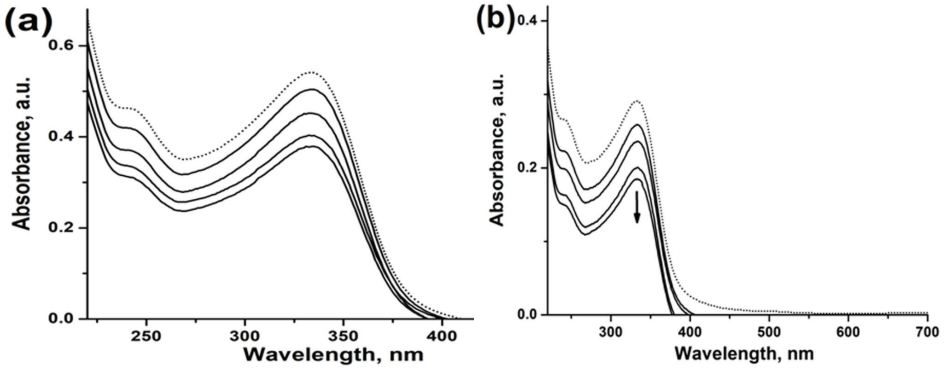

Fig. 2. Absorption spectra of complexes **1** (a) and **2** (b) in Tris-HCl/NaCl buffer at room temperature in the presence of CT-DNA solutions. Dotted lines refer to the free compound; the solid lines to absorption spectra of the compound in the presence of different concentrations of DNA.

The K_b values were obtained from the ratio of slope to the intercept from plots of $c_{DNA}/(\varepsilon_a–\varepsilon_f)$ *vs.* c_{DNA}. The obtained K_b values of the synthesized compounds (2.65×10^3, **L**; 7.74×10^3, **1** and 2.99×10^3, **2**) are given in Table IV. The obtained K_b values are low as compared to that for ethidium bromide (EB) (1.4×10^6). The lower K_b values for synthesized compounds are due to the flexible, versatile morpholine moiety in the complexes that greatly facilitate

TABLE IV. Absorption spectral properties of the synthesized compounds on interaction with CT-DNA

Compound	λ_{max} / nm		$\Delta\lambda$ / nm	Hypochromism, %	K_b / 10^3
	Free	Bound			
1	329.0	335.0	6.0	15.60	7.74
2	338.0	343.0	5.0	13.57	2.99
L	336.0	339.0	3.0	6.27	2.65

intercalation with the base pairs. The binding strengths of the studied compounds with DNA show that complex **1** has a higher binding affinity as compared to ligand **L** and complex **2**, in the following order: **1** > **2** > **L**.

Competitive binding. The fluorescence spectra of EB–DNA in the presence of the prepared compounds are presented in Fig. 3. As shown in Fig. 3a and b, the concentration of complexes **1** and **2** enlarges to the EB–DNA, the fluorescence intensity of the complexes **1** and **2** steadily decreases. These results confirm that competitive interactions occurred. The intercalative binding of ligand **L**, complexes **1** and **2** with EB–DNA could be summarized by the Stern–Volmer equation:[44]

$$I_0/I = 1 + K_{sv}c_Q \quad (3)$$

where I and I_0 are the emission intensities in the presence and absence of the quenchers (ligand **L**, complexes **1** and **2**), respectively, K_{sv} is the linear Stern–Volmer quenching constant and c_Q is the concentration of the quencher. The K_{sv} values were obtained from the slope of plots of I_0 / I *vs.* c_Q (Fig. 3). Additionally, the binding affinity (K_{app}) of ligand **L** complexes **1** and **2** in contrast to that of EB was evaluated using the following equation:[45]

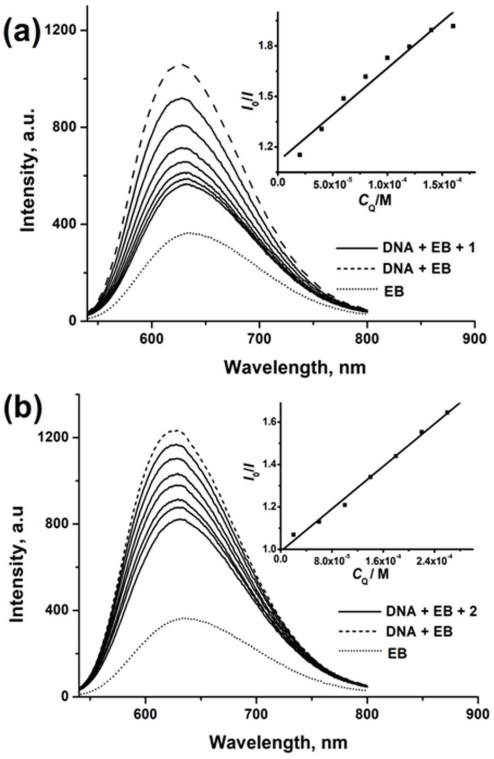

Fig. 3. Emission spectra of EB–CT-DNA in the presence of increasing amounts of complex **1** (a) and **2** (b).

$$K_{EB}c_{EB} = K_{app}c_{complex} \quad (4)$$

where, $c_{complex}$ is the concentration of the newly prepared compounds necessary for a 50 % reduction in the fluorescence intensity of EB and $K_{EB} = 1.0\times10^7$. The binding constant (K_{sv}) and binding affinity (K_{app}) values of the present compounds are given in Table V. The K_{sv} and K_{app} values of the prepared compounds are in the following order: **1** (K_{sv} 4.31×10^3 and K_{app} 3.30×10^5) > **2** (K_{sv} 3.89×10^3 and K_{app} 2.82×10^5) > **L** (K_{sv} 3.30×10^3 and K_{app} 2.15×10^5).

TABLE V. The quenching constants and binding affinity of ligand **L**, and complexes **1** and **2** with EB–DNA

Compound	K_{sv} / 10^3	K_{app} / 10^5
1	4.31	3.30
2	3.89	2.82
L	3.30	2.15

Electrochemical studies

The results of cyclic voltammetric measurements of complexes **1** and **2** in the presence and absence of CT-DNA (0–50 μM) are presented in Fig. 4a and b. Here, as the concentration of CT-DNA rises, the cathodic and anodic peak currents of the prepared complexes **1** and **2** increase, and their peak potentials are shifted to negative values. These findings confirm that the newly prepared compounds can interact with CT-DNA.

Viscosity measurements

The viscometric studies were very useful in the clarification of the nature of the binding of the synthesized compounds to CT-DNA. The graphs of the relative viscosity *vs*. $c_{complex}/c_{DNA}$ are presented in Fig. 5. As the concentration of compounds increases, the viscous flow of CT-DNA increases. These results correlate

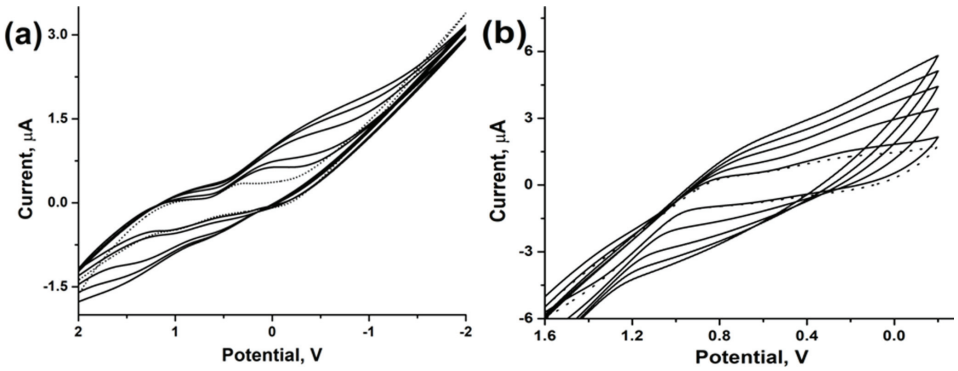

Fig. 4. Cyclic voltammograms of complexes **1** (a) and **2** (b) in Tris-HCl buffer at 25 °C in the presence of increasing amounts of CT-DNA.

with the spectroscopic and cyclic voltammetric results that suggested the prepared compounds should interact with CT-DNA through an intercalation mode.

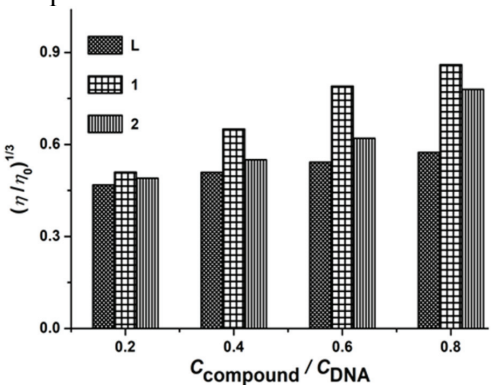

Fig. 5. Effect of increasing amount of complexes **1** and **2** on the relative viscosity of DNA. $1/R = c_{compound}/c_{DNA}$.

CONCLUSION

The Schiff base ligand **L**, and complexes **1** and **2** were isolated from pyrimidine backbones. The analytical data confirmed that the prepared complexes **1** and **2** possess 1:2 stoichiometry ratios. Square planar geometry of complexes **1** and **2** were finalized from the results of spectroscopic techniques. The prepared compounds possess better antibacterial and antifungal activity against *E. coli* (bacteria) and *C. albicans* (fungi) than against the other tested pathogenic species. The molecular docking results revealed that ligand **L** can interact with proteins. The interacting ability of ligand **L**, and complexes **1** and **2** with CT-DNA were explored by spectroscopic, cyclic voltammetric and viscometric techniques and the results suggested that the prepared complexes can bind with CT-DNA by intercalatation. The *in vitro* antitumor results suggested that the pyrimidine incorporating complexes **1** and **2** have moderate anticancer activities.

SUPPLEMENTARY MATERIAL

Spectral and analytical data of the synthesized compounds, as well as graphical representation of anticancer activities, are available electronically at the pages of journal website: http://www.shd.org.rs/JSCS/, or from the corresponding author on request.

Acknowledgements. The authors acknowledge the Department of Science and Technology (DST)-Science and Engineering Research Board (SERB-Ref. No.: SR/FT/CS-117/2011 dated 29.06.2012), Government of India, New Delhi for the financial support. The authors express their sincere and heartfelt thanks to Managing Board, Dean, Principal, Head and staff members, Chemistry Research Centre, Mohamed Sathak Engineering College, Kilakarai for their constant encouragement and providing the research facilities.

ИЗВОД

КОМПЈУТЕРСКА АНАЛИЗА, ДНК ИНТЕРАКЦИЈЕ, АНТИМИКРОБНА И АНТИКАНЦЕРСКА АКТИВНОСТ БАКАР(II) И ЦИНК(II) КОМПЛЕКСА СА ЛИГАНДОМ КОЈИ САДРЖИ ПИРИМИДИНСКИ ПРСТЕН

MURUGESAN SANKARGANESH[1], NAGARAJ REVATHI[2,3], JEYARAJ DHAVEETHU RAJA[1], KARUNGANATHAN SAKTHIKUMAR[1], GUJULUVA GANGATHARAN VINOTH KUMAR[1], JEGATHALAPRATHABAN RAJESH[1], MANIKKAM RAJALAKSHMI[4] и LIVIU MITU[5]

[1]Chemistry Research Centre, Mohamed Sathak Engineering College, Kilakarai, Ramanathapuram, Tamil Nadu 623 806 India, [2]Department of Chemistry, Ramco Institute of Technology, Rajapalayam, Virudhunagar, Tamil Nadu 626 117, India, [3]Department of Chemistry, Manonmanium Sundaranar University, Tirunelvi, Tamil Nadu 627 012, India, [4]Bioinformatics Centre, PG & Research Centre Department of Biotechnology and Bioinformatics, Holy Cross College (Autonomous), Tiruchirapalli, Tamil Nadu 620 002, India и [5]Department of Nature Sciences, University of Pitesti, Pitesti 110 040, Romania

У овом раду описана је синтеза, структурна карактеризација, антимикробна и антиканцерска својства, као и испитивање интеракција са молекулом ДНК, комплекса $[CuL_2]\cdot(ClO_4)_2$ (**1**) и $[ZnL_2]\cdot(ClO_4)_2$ (**2**) који као лиганд (**L**) садрже Шифову базу. У односу на лиганд, одговарајући комплекси (**1** и **2**) су показали значајну антибактеријску и антифунгалну активност. На основу електронских апсорпционих, флуорометријских и циклично-волтаметријских мерења, као и на основу мерења вискозитета, потврђено је интеркалативно везивање комплекса за хеликс ДНК. Израчунати су следећи параметри везивања испитиваних комплекса за ДНК: K_b (2.65×10^3 (**L**); 7.74×10^3 (**1**) и 2.99×10^3 (**2**)), K_{sv} (3.30×10^3 (**L**); 4.31×10^3 (**1**) и 3.89×10^3 (**2**)) и K_{app} (2.15×10^5 (**L**); 3.30×10^5 (**1**) и 2.82×10^5 (**2**)). Ове вредности показују да комплекс **1** има бољу интеркалациону способност везивања за ДНК у односу на лиганд **L** и комплекс **2**. *In vitro* антиканцерска својства лиганда **L** и комплекса **1** и **2** према хуманим ћелијама тумора (MCF-7, HeLa и HEp-2) и нормалним (NHDF) ћелијским линијама одређена су помоћу MTT методе. Добијени резултати су показали да комплекси **1** и **2** показују значајно већу активност према ћелијама канцера у односу на лиганд **L**.

(Примљено 6. јуна, ревидирано 7. августа, прихваћено 5. септембра 2018)

REFERENCES

1. R. C. Reynolds, A. Tiwari, J. E. Harwell, D. G. Gordon, B. D. Garrett, K. S. Gilbert, S. M. Schmid, W. R. Waud, R. F. Struck, *J. Med. Chem.* **43** (2000) 1484 (https://doi.org/10.1021/jm990417j)
2. S. A. F. Rostom, H. M. A. Ashour, H. A. Abdel Razik, *Arch. Pharm.* **342** (2009) 299 (https://doi.org/10.1002/ardp.200800223)
3. H. Parveen, F. Hayat, A. Salahuddin, A. Salahuddin, A. Azam, *Eur. J. Med. Chem.* **45** (2010) 3497 (https://doi.org/10.1016/j.ejmech.2010.04.023)
4. C. Sirichaiwat, C. Intaraudom, S. Kamchonwongpaisan, J. Vanichtanankul, Y. Thebtaranonth, Y. Yuthavong, *J. Med. Chem.* **47** (2004) 345 (https://doi.org/10.1021/-jm0303352)
5. S. Kamchonwongpaisan, R. Quarrell, N. Charoensetakul, R. Ponsinet, T. Vilaivan, J. Vanichtanankul, B. Tarnchompoo, W. Sirawaraporn, G. Lowe, Y. Yuthavong, *J. Med. Chem*. **47** (2004) 673 (https://doi.org/10.1021/jm030165t)
6. D. W. Boykin, A. Kumar, M. Baji, G. Xiao, W. D. Wilson, B. C. Bender, D. R. McCurdy, J. E. Hall, R. R. Tidwell, *Eur. J. Med. Chem*. **32** (1998) 965 (https://doi.org/10.1016/-s0223-5234(97)89640-7)

7. S. F. Chowdhury, V. B. Villamor, R. H. Guerrero, I. Leal, R. Brun, S. L. Croft, J. M. Goodman, L. Maes, L. M. Ruiz-Perez, D. G. Pacanowska, I. H. Gilbert, *J. Med. Chem*. **42** (1999) 4300 (https://doi.org/10.1021/jm981130)
8. M. S. S. Palanki, P. E. Erdman, L. M. G. Fung, G. I. Shevlin, R. W. Sullivan, M. E. Goldman, L. J. Ransone, B. L. Bennett, A. M. Manning, M. J. Suto, *J. Med. Chem*. **43** (2000) 3995 (https://doi.org/10.1021/jm0001626)
9. P. Bravo, D. Diliddo, G. Resnati, *Tetrahedron* **50** (1994) 8827 (https://doi.org/10.1016/-s0040-4020(01)85356-4)
10. J. C. Jung, E. B. Watkins, M. A. Avery, *Tetrahedron* **58** (2002) 3639 (https://doi.org/-10.1016/S0040-4020(02)00306-X)
11. K. L. Kees, J. J. Fitzgerald, K. E. Steiner, J. F. Mattes, B. Mihan, T. Tosi, D. Mondoro, M. L. McCaleb, *J. Med. Chem*. **39** (1996) 3920 (https://doi.org/10.1021/jm960444z)
12. G. T. Payne, D. C. Deecher, D. M. Soderlund, *Pestic Biochem. Physiol.* **60** (1998) 177 (https://doi.org/10.1006/pest.1998.2350)
13. S. G. Kucukguzel, S. Rollas, H. Erdeniz, M. Kiranz, A. C. Ekinci, A. Vidin, *Eur. J. Med. Chem*. **35** (2000) 761 (https://doi.org/10.1016/s0223-5234(00)90179-x)
14. M. Burotto, E. E. Manasanch, J. Wilkerson, T. Fojo, *Oncologist* **20** (2015) 400 (https://doi.org/10.1634/theoncologist.2014-0154)
15. M. S. El-Shahawi, M. S. Al-Jahdali, A. S. Bashammakh, A. A. Al-Sibaai, H. M. Nassef, *Spectrochim. Acta, A* **113** (2013) 459 (https://doi.org/10.1016/j.saa.2013.04.090)
16. A. H. Osman, *Transition Met. Chem*. **31** (2006) 35 (https://doi.org/10.1007/s11243-005-6265-7)
17. A. H. Osman, M. S. Saleh, S. M. Mahmoud, *Synth. React. Inorg. Met. - Org. Chem*. **34** (2004) 1069 (https://doi.org/10.1081/sim-120039258)
18. P. R. Inamdar, A. Sheela, *Int. J. Biol. Macromol*. **76** (2015) 269 (https://doi.org/-10.1016/j.ijbiomac.2015.02.027)
19. B. Balaji, B. Balakrishnan, S. Perumalla, A. A. Karande, A. R. Chakravarty, *Eur. J. Med. Chem*. **85** (2014) 458 (https://doi.org/10.1016/j.ejmech.2014.07.098)
20. A. Sheela, S. M. Roopan, R. Vijayrahavan, *Eur. J. Med. Chem*. **43** (2008) 2206 (https://doi.org/10.1016/j.ejmech.2008.01.002)
21. M. Sankarganesh, J. Rajesh, G. G. Vinoth Kumar, M. Vadivel, L. Mitu, R. Senthil Kumar, J. Dhaveethu Raja, *J. Saudi Chem. Soc*. **22** (2018) 416 (https://doi.org/10.1016/-j.jscs.2017.08.007)
22. J. W. Liang, Y. Wang, K. J. Du, G. Y. Li, R. L. Guan, L. N. Ji, H. Chao, *J. Inorg. Biochem*. **141** (2014) 17 (https://doi.org/10.1016/j.jinorgbio.2014.08.006)
23. S. Yasmin, S. Rabi, F. B. Biswas, T. G. Roy, F. Olbrich, D. Rehder, *J. Inclusion Phenom. Macrocyclic Chem.* **87** (2017) 239 (https://doi.org/10.1007/s10847-017-0693-9)
24. *Gaussian 09, Revision A.02*, Gaussian, Inc., Wallingford CT, 2009
25. N. Revathi, M. Sankarganesh, J. Rajesh, J. Dhaveethu Raja, *J. Fluoresc.* **27** (2017) 1801 (https://doi.org/10.1007/s10895-017-2118-y)
26. R. Arunkumara, G. Sharmilaa, P. Elumalaia, K. Senthilkumara, S. Banudevia, D. N. Gunadharinia, C. S. Bensona, P. Daisyb, J. Arunakarana, *Phytomedicine* **19** (2012) 912 (http://dx.doi.org/10.1016/j.phymed.2012.04.000)
27. M. Sankarganesh, P. Adwin Jose, J. Dhaveethu Raja, M. P. Kesavan, M. Vadivel, J. Rajesh, R. Jeyamurugan, R. Senthil Kumar, S. Karthikeyan, *J. Photochem. Photobiol., B* **176** (2017) 44 (https://doi.org/10.1016/j.jphotobiol.2017.09.013)
28. A. Gubendran, M. P. Kesavan, S. Ayyanaar, J. Dhaveethu Raja, P. Athappan, J. Rajesh, *Appl. Organomet. Chem*. **31** (2017) e3708 (https://doi.org/10.1002/aoc.3708)

29. S. Chandra, L. K. Gupta, *Spectrochim. Acta, Part A* **60** (2004) 1563 (https://doi.org/10.1016/j.saa.2004.01.015)
30. R. M. Silverstein, G. C. Bassler, T. C. Morrill, *Spectrometric Identification of Organic Compounds*, 4th ed., Wiley, New York, 1981
31. A. B. P. Lever, *Inorganic Electronic Spectroscopy*, Elsevier, Amsterdam, 1984
32. C. Ballhausen, *Ligand field theory*, McGraw Hill, New York, 1962
33. M. B. Halli, R. B. Sumathi, M. Kinni, *Spectrochim. Acta, Part A* **99** (2012) 46 (https://doi.org/10.1016/j.saa.2012.08.089)
34. N. Raman, A. Sakthivel, J. Dhaveethu Raja, K. Rajasekaran, *Russ. J. Inorg. Chem*. **53** (2008) 213 (https://doi.org/10.1134/s0036023608020113)
35. N. Raman, L. Mitu, A. Sakthivel, M. S. S. Pandi, *J. Iran. Chem. Soc*. **6** (2009) 738 (https://doi.org/10.1007/bf03246164)
36. N. Raman, J. Dhaveethu Raja, A. Saktivel, *J. Chem. Sci*. **119** (2007) 303 (https://doi.org/10.1007/s12039-007-0041-5)
37. R. L. Dutta, A. Syamal, *Elements of Magnetochemistry*, Affiliated East-West Press, New Delhi, 1993
38. B. J. Hathaway, D. E. Billing, *Coord. Chem. Rev.* **5** (1970) 143 (https://doi.org/-10.1016/s0010-8545(00)80135-6)
39. H. Montgomery, E. C. Lingefetter, *Acta Crystallogr*. **20** (1966) 728 (https://doi.org/-10.1107/s0365110x66001750)
40. A. M. F. Benial, V. Ramakrishnan, R. Murugesan *Spectrochim. Acta, A* **56** (2000) 2775 (https://doi.org/10.1016/s1386-1425(00)00322-x)
41. N. Raman, S. S. A. Fathima, J. Dhaveethu Raja, *J. Serb. Chem. Soc*. **73** (2008) 1063 (https://doi.org/10.2298/jsc0811063r)
42. P. Daisy, S. Suveena, V. Lilly Sr., *J. Chem. Pharm. Res*. **3** (3) (2011) 557 (http://www.jocpr.com/articles/molecular-docking-of-medicinal-compound-lupeol-with-autolysin-and-potential-drug-target-of-uti.pdf)
43. P. Daisy, P. Vijayalakshmi, C. Selvaraj S. K. Singh, K. Saipriya, *Indian J. Pharm. Sci*. **74** (2012) 217 (https://doi.org/10.4103/0250-474x.106063)
44. P. Adwin Jose, J. Dhaveethu Raja, M. Sankarganesh, J. Rajesh, *J. Photochem. Photobiol., B* **178** (2018) 143 (https://doi.org/10.1016/j.jphotobiol.2017.11.005)
45. S. M. Kumar, M. P. Kesavan, G. G. Vinoth Kumar, M. Sankarganesh, G. Chakkaravarthi, G. Rajagopal, J Rajesh, *J. Mol. Struct.* **1153** (2018) 1 (https://doi.org/10.1016/j.mol-struc.2017.09.070).